sidered to be negligible. ^{13}C chemical shifts were referenced to the signal of the solvent, THF-d_8, α-C = 67.4 ppm. ^{1}H chemical shifts were referenced to the residual solvent signal, THF-d_7, α-H = 3.58 ppm. Deuterium lock on THF-d_8 was obtained by using the upfield (β-D) signal of the solvent. We found this to be more convenient than using the α-D signal since the β-deuterium resonance line appears to be generally sharper. This is beneficial for the shimming procedure.

All 2D NMR spectra were recorded in the phase-sensitive mode (pure absorption quadrature detection in f_1 by the method described by States et al.[69]). Details of phase-sensitive ^{6}Li,^{1}H HOESY[33] and ^{133}Cs,^{1}H HOESY[37] have been described elsewhere. Selected recording parameters of the individual spectra were as follows.

For the spectrum in Figure 1 (^{6}Li,^{1}H HOESY of 8): 0.35 M solution in THF-d_8 (dissolved crystals of [^{6}Li]lithium trityl with 2 equiv of Et$_2$O), 26 °C, 5-mm sample tube; spectral widths: 400 (f_2) and 3157 Hz (f_1); 512 data points in t_2, 32 increments in t_1, zero-filled to 128 data points, exponential line broadening in t_2, Gaussian apodization in t_1; 128 scans per t_1 increment, mixing time 2.0 s, interpulse delay 3.0 s, 12.8 h spectrometer time.

For the spectrum in Figure 2 (^{133}Cs,^{1}H HOESY of 9): 1.2 M solution in THF-d_8 (dissolved crystals of 9), 40 °C, 5-mm sample tube; spectral widths: 14006 (f_2) and 364 Hz (f_1); 512 data points in t_2, 32 increments in t_1, zero-filled to 128 data points, Gaussian apodization in t_1 and t_2, 256 scans per t_1 increment; mixing time 300 ms. A crude estimation of the spin lattice relaxation time, T_1, of ^{133}Cs afforded $T_1 \approx 400$ ms (achieved by null point determination in a single inversion recovery experiment, divided by ln 2); interpulse delay 2.1 s, 11.0 h spectrometer time.

For the spectrum in Figure 3 (^{6}Li,^{1}H HOESY of a mixture of 8 and 9): Crystals of 8 (enriched with ^{6}Li and with 2 equiv of Et$_2$O) and crystals of 9 dissolved in THF-d_8, 1:1.5 molar ratio, 0.6 M in 8, 26 °C, 10-mm sample tube; spectral widths: 400 (f_2) and 3270 Hz (f_1); 512 data points in t_2, 64 increments in t_1, zero-filled to 256 points; exponential line broadening in t_2, Gaussian apodization in t_1; mixing time 2.0 s, interpulse delay 3.2 s, 13.3 h spectrometer time.

For the spectrum in Figure 4 (^{133}Cs,^{1}H HOESY of a mixture of 8 and 9): Crystals of 8 (enriched with ^{6}Li and with 2 equiv of Et$_2$O) and crystals of 9 dissolved in THF-d_8, 1.2:1 molar ratio, 0.6 M in 8, 26 °C, 10-mm sample tube; spectral widths: 1600 (f_2) and 3270 Hz (f_1); 512 data points in t_2, 16 increments in t_1, zero-filled to 128 points, Gaussian apodization in t_1 and t_2, 640 scans per t_1 increment; mixing time 350 ms (an estimation afforded $T_1(^{133}$Cs) $\approx$ 370 ms; see explanation given above for Figure 2); interpulse delay 3.2 s, 21 h spectrometer time.

For the spectrum in Figure 5 (^{1}H,^{1}H ROESY of a mixture of 8 and 9): Crystals of 8 (enriched with ^{6}Li and with 2 equiv of Et$_2$O) and crystals of 9 dissolved in THF-d_8, 1:1.5 molar ratio, 0.6 M in 8, 20 °C; spectral width 3270 Hz; pulse sequence 90°–t_1–(12.6-μs pulse–126-μs delay)$_{7200}$–acquisition–delay;[70] 2048 data points in t_2, 128 increments in t_1, zero-filled to 256 data points; 64 scans per t_1 increment, Gaussian apodization in t_1 and t_2; spin lock time 1.0 s, interpulse delay 2.0 s, 4.6 h spectrometer time.

MNDO calculations were carried out on a CONVEX C220 computer using the VAMP4 (vectorized AMPAC) program. All geometry optimizations involved the keywords PRECISE (criteria for convergence to be increased by a factor of 10–100) or EF (eigenvector following). No symmetry constraints were imposed in any case.

(69) States, D. J.; Haberkorn, R. A.; Ruben, D. J. *J. Magn. Reson.* **1982**, *48*, 286.

(70) Kessler, H.; Griesinger, C.; Kerssebaum, R.; Wagner, K.; Ernst, R. R. *J. Am. Chem. Soc.* **1987**, *109*, 607.

^{87}Rb Dynamic-Angle Spinning NMR Spectroscopy of Inorganic Rubidium Salts

J. H. Baltisberger, S. L. Gann, E. W. Wooten,[†] T. H. Chang,[‡] K. T. Mueller,[§] and A. Pines*

Contribution from the Materials Sciences Division, Lawrence Berkeley Laboratory, 1 Cyclotron Road, Berkeley, California 94720, and Department of Chemistry, University of California, Berkeley, California 94720. Received April 1, 1992

Abstract: Five inorganic rubidium salts, RbCl, RbClO$_4$, Rb$_2$SO$_4$, Rb$_2$CrO$_4$, and RbNO$_3$, were examined using ^{87}Rb NMR spectroscopy. Significant line narrowing occurs under dynamic-angle spinning (DAS) compared to magic-angle spinning (MAS) or variable-angle spinning (VAS). From DAS spectra acquired at various magnetic field strengths, isotropic chemical shifts and isotropic second-order quadrupolar shifts were obtained. By simulations of single-site line shapes obtained from MAS-detected DAS experiments, complete chemical shift and quadrupolar parameters were determined for each of the three crystallographically distinct rubidium sites in RbNO$_3$.

Introduction

Solid-state nuclear magnetic resonance (NMR) spectroscopy of the central ($-^1/_2 \leftrightarrow +^1/_2$) transition of half-odd-integer quadrupolar nuclei can yield information about the nuclear quadrupole interaction, which in turn can be correlated with the

structural properties of a material.[1,2] Typically, though, the spectral line from the central transition is broadened by the second-order anisotropic quadrupolar interaction, which cannot be averaged under magic-angle spinning (MAS) or variable-angle spinning (VAS). Recent work has shown, however, that dynamic-angle spinning (DAS) can average such broadening, producing narrow lines and resolution of crystallographically distinct sites for ^{23}Na, ^{17}O, and ^{27}Al spectra of minerals, zeolites, and other

* To whom correspondence should be addressed at the University of California.
† Current address: Biophysics Research Division, The University of Michigan, Ann Arbor, MI 48109.
‡ Current address: Industrial Technology Research Institute, Union Chemical Laboratories, Hsin Chu, Taiwan, ROC.
§ Current address: Department of Chemistry, University of British Columbia, Vancouver, BC V6T 1Y6, Canada.

(1) Tossel, J. A.; Lazzeretti, P. *Phys. Chem. Miner.* **1988**, *15*, 564–569.
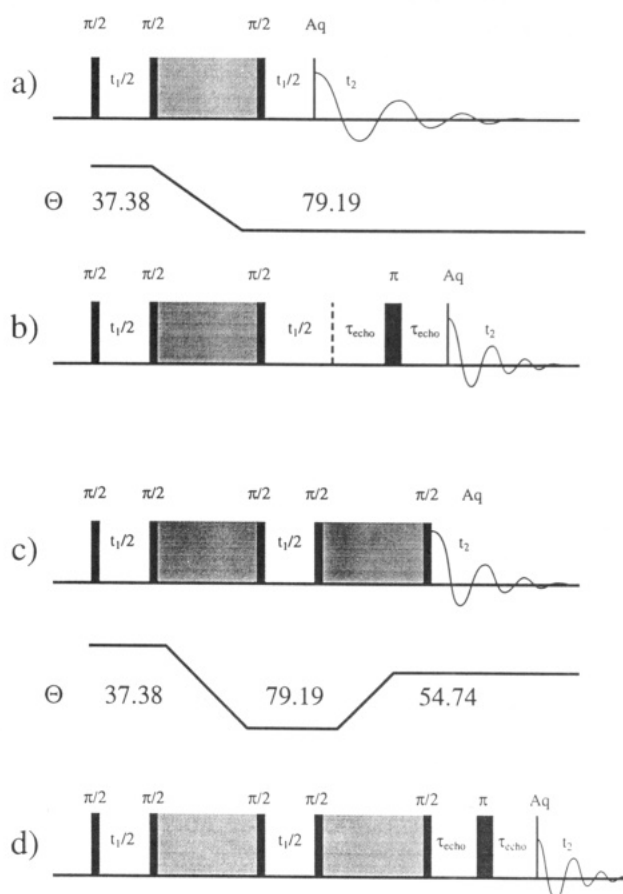(2) Kirkpatrick, R. J. In *Spectroscopic Methods in Mineralogy and Geology*; Hawthorne, F. C., Ed.; Reviews in Mineralogy; Mineralogical Society of America: Washington, DC, 1988; Vol. 18, pp 341–403.

inorganic materials.[3-5] In this paper, we extend our previous NMR investigations of half-odd-integer quadrupolar nuclei to ^{87}Rb ($I = ^3/_2$). Alkali metals such as rubidium are important in a number of areas, serving as promoters in the heterogeneous catalysis of ammonia synthesis[6] and the oxidative coupling of methane to yield ethane and ethene.[7] Rubidium is an important component of some glasses,[8] and recently, it has been shown that buckminsterfullerene, C_{60}, doped with Rb metal becomes superconducting with a transition temperature at 28 K.[9]

In order to assess the applicability of dynamic-angle spinning NMR spectroscopy to rubidium and its potential to yield structural information about materials such as those listed above, we have obtained ^{87}Rb MAS, VAS, and DAS spectra of five inorganic rubidium salts, RbCl, $RbClO_4$, Rb_2SO_4, Rb_2CrO_4, and $RbNO_3$. We show that substantial narrowing of the spectral lines occurs in DAS compared to MAS or VAS. Using pure-phase MAS-detected DAS experiments together with single-site simulations and phase-modulated DAS experiments at several field strengths, we have extracted quadrupolar parameters for the various ^{87}Rb sites in each compound. The static line shapes of all of these compounds have previously been studied by Cheng et al.[10] in order to obtain values for quadrupolar and chemical shift parameters. Crystal structures for all of the compounds RbCl,[11] $RbClO_4$,[12] Rb_2CrO_4,[13] Rb_2SO_4,[14] and $RbNO_3$[15,16] have also been previously determined and are used to identify the number of inequivalent sites in each compound.

Experimental Section

All rubidium compounds were obtained from Alfa Products, Morton Thiokol, Inc., or Aldrich Chemical Co. and used without further purification. Experimental details of the DAS experiment have been reported previously.[3,17,18] Spectra were acquired at 4.2 T (58.80 MHz), 7.0 T (98.55 MHz), 9.4 T (130.89 MHz), and 11.7 T (163.62 MHz) using the probe design described in ref 18 and the pulse sequences and rotor orientations shown in Figure 1.[3,17] The pulse sequences shown in Figure 1a,b were used to collect phase-modulated data sets, while the sequences in Figure 1c,d gave phase-sensitive data sets and allowed t_2 detection at the magic angle. Phase-sensitive data were acquired using either TPPI,[19,20] in which the phase of the first pulse is shifted by $\pi/2$ in concert with t_1, or the method of States et al.,[21] in which data from two experiments with t_1 modulations differing in phase by $\pi/2$ are combined. The two experiments required by the method of States et al. are in addition to the two experiments needed for the reconstruction of the second-order echo in DAS.[17] Pure-phase t_1 projections from phase-modulated data sets were produced as detailed in ref 17. The pulse sequences used at 11.7

(3) Mueller, K. T.; Sun, B. Q.; Chingas, G. C.; Zwanziger, J. W.; Terao, T.; Pines, A. *J. Magn. Reson.* **1990**, *86*, 470–487.

(4) Mueller, K. T.; Baltisberger, J. H.; Wooten, E. W.; Pines A. *J. Phys. Chem.*, in press.

(5) Wu, Y.; Chmelka, B. F.; Pines, A.; Davis, M. E.; Grobet, P. J.; Jacobs, P. A. *Nature* (*London*) **1990**, *346*, 550–552.

(6) Hikita, T.; Aika, K.; Onishi, T. *Catal. Lett.* **1990**, *4*, 157–162.

(7) Aika, K.; Fujimoto, N.; Kobayashi, M.; Iwamatsu, E. *J. Catal.* **1991**, *127*, 1–8.

(8) Bansal, N. P.; Doremus, R. H. *Handbook of Glass Properties*; Academic Press, Inc.: Orlando, FL, 1986.

(9) Rosseinsky, M. J.; Ramirez, A. P.; Glarum, S. H.; Murphy, D. W.; Haddon, R. C.; Hebard, A. F.; Palstra, T. T. M.; Kortan, A. R.; Zahurak, S. M.; Makhija, A. V. *Phys. Rev. Lett.* **1991**, *66*, 2830–2832.

(10) Cheng, J. T.; Edwards, J. C.; Ellis, P. D. *J. Phys. Chem.* **1990**, *94*, 553–561.

(11) Deshpande, V. T.; Sirdeshmukh, D. B. *Acta Crystallogr.* **1961**, *14*, 353–355.

(12) Braeken, H.; Harang, L. *Z. Kristallogr.* **1930**, *75*, 538–549.

(13) Smith, H. W.; Colby, M. Y. *Z. Kristallogr.* **1940**, *103*, 90–95.

(14) Nord, A. G. *Acta Crystallogr.* **1974**, *B30*, 1640–1641.

(15) Shamsuzzoha, M.; Lucas, B. W. *Acta Crystallogr.* **1982**, *B38*, 2353–2357.

(16) Dean, C.; Hambley, T. W.; Snow, M. R. *Acta Crystallogr.* **1984**, *C40*, 1512–1515.

(17) Mueller, K. T.; Wooten, E. W.; Pines, A. *J. Magn. Reson.* **1991**, *92*, 620–627.

(18) Mueller, K. T.; Chingas, G. C.; Pines, A. *Rev. Sci. Instrum.* **1991**, *62*, 1445–1452.

(19) Drobny, G.; Pines, A.; Sinton, S.; Weitekamp, D.; Wemmer, D. *Symp. Faraday Soc.* **1979**, *13*, 49–55.

(20) Marion, D.; Wüthrich, K. *Biochem. Biophys. Res. Commun.* **1983**, *113*, 967–974.

(21) States, D. J.; Haberkorn, R. A.; Ruben, D. J. *J. Magn. Reson.* **1982**, *48*, 286–292.

Figure 1. DAS pulse sequences used for these experiments: (a) phase-modulated DAS;[3] (b) phase-modulated DAS with Hahn echo; (c) phase-sensitive DAS;[17] (d) phase-sensitive DAS with Hahn echo. The spinner axis angles are indicated by the θ curves between both types of sequences.

T were modified by inserting a $\tau-\pi-\tau$ sequence before the detection period with τ equal to the inverse of the spinning speed (Figure 1b,d). Detection of the resulting echo minimizes the effects of receiver ringdown. The ^{81}Br signal in solid KBr was used as an internal standard for calibration of the magic angle. All spectra are referenced relative to aqueous 1 M $RbNO_3$ as an external frequency standard. Either 256 or 512 complex points were acquired in t_2, and between 128 and 512 real points, in t_1. Spectra were acquired with 1.0 s relaxation delays and $\pi/2$ pulses selective for the central transition of approximately 5 μs ($B_1 \sim$ 20 G). Hopping times for the reorientation of the rotor axis as shown in Figure 1 were about 30 ms. Normal rotor-spinning speeds were between 6.5 and 7.8 kHz.

All VAS, MAS, and static spectra were acquired using a Hahn echo pulse sequence ($\pi/2-\tau-\pi-\tau-acquire$). T_1 measurements were made using an inversion–recovery sequence under MAS. T_2 was measured using a Carr–Purcell sequence under MAS. Double-rotation (DOR) experiments were performed at 9.4 T as described previously[4,5] in order to determine the DOR line width.

Calculations. Calculations of quadrupolar shifts and parameters were performed using the field dependence of the isotropic shifts as described in ref 4. The total isotropic shift (ppm) in the F_1 dimension of a DAS experiment is given by

$$\delta_{obs} = \delta_{iso}^{(CS)} + \delta_{iso}^{(2)} \qquad (1)$$

where $\delta_{iso}^{(CS)}$ is the isotropic chemical shift and $\delta_{iso}^{(2)}$ is the isotropic second-order quadrupolar shift. The isotropic chemical shift in ppm is frequency independent, while the isotropic second-order quadrupolar shift in ppm for a spin I depends upon the Larmor frequency (ν_L):

$$\delta_{iso}^{(2)} = -\frac{3 \times 10^6}{40} \frac{C_Q^2(I(I+1) - \frac{3}{4})}{\nu_L^2 I^2 (2I-1)^2} \left(1 + \frac{\eta^2}{3}\right) \qquad (2)$$

The quadrupolar coupling constant is defined by

$$C_Q \equiv \frac{e^2 qQ}{h} \qquad (3)$$

[87]Rb NMR Spectroscopy of Inorganic Rubidium Salts

J. Am. Chem. Soc., Vol. 114, No. 19, 1992 7491

Table I. Coefficients in the Anisotropic Frequency Cosine Expansion

i	j	a_{ij}	i	j	a_{ij}
0	0	$81(18 + \eta^2)/1120$	1	2	$-27\eta/8$
0	1	$9(18 + \eta^2)/56$	2	0	$27\eta^2/32$
0	2	$9(18 + \eta^2)/32$	2	1	$-9\eta^2/8$
1	0	$81\eta/56$	2	2	$9\eta^2/32$
1	1	$27\eta/14$			

Table II. Results from DAS Experiments at 9.4 and 11.7 T[a]

compd	$\delta_{obs}^{9.4T}$ (ppm)	$\delta_{obs}^{11.7T}$ (ppm)	$\delta_{iso}^{(CS)}$ (ppm)	$C_Q(1 + \eta^2/3)^{1/2}$ (MHz)
RbCl	127 ± 1	127 ± 1	127 ± 2	~ 0
RbClO$_4$	-28 ± 1	-23 ± 1	-14 ± 2	3.1 ± 0.3
Rb$_2$SO$_4$	-25 ± 1	-10 ± 1	16 ± 2	5.3 ± 0.2
	29 ± 1	34 ± 1	42 ± 2	3.0 ± 0.3
Rb$_2$CrO$_4$	-27 ± 1	-21 ± 1	-11 ± 2	3.3 ± 0.3
	b	b	b	b
RbNO$_3$	-32 ± 1	-29 ± 1	-24 ± 2	2.4 ± 0.4
	-36 ± 1	-32 ± 1	-25 ± 2	2.8 ± 0.4
	-37 ± 1	-34 ± 1	-29 ± 2	2.4 ± 0.4

[a] The isotropic chemical shift and product of quadrupolar parameters were calculated using eq 4. [b] This site was too broad for detection in the DAS and MAS experiments.

The quantities eQ (1.3×10^{-29} m^2 for [87]Rb), eq, η, and h have their usual definitions.[4] Using eqs 1 and 2, we can calculate $\delta_{iso}^{(CS)}$ and the product $C_Q(1 + \eta^2/3)^{1/2}$ if we measure the total isotropic shift (δ_{obs}) at two different field strengths. In addition, if isotropic shifts are known for three or more field strengths, significant improvement in both the accuracy and the precision of $C_Q(1 + \eta^2/3)^{1/2}$ and $\delta_{iso}^{(CS)}$ may be achieved using a linear least squares analysis of the data with the following equation for [87]Rb:

$$\delta_{obs} = \delta_{iso}^{(CS)} - \left(1.28 \times 10^{-10} \frac{T^2}{Hz^2}\right)[C_Q(1 + \eta^2/3)^{1/2}]^2 \left(\frac{1}{B_0^2}\right) \quad (4)$$

We cannot, however, determine the individual values of C_Q and η using calculations; to do that, we must perform simulations.

Simulations. Single-site MAS spectra were obtained from the phase-sensitive MAS-detected DAS data set by extracting the individual columns in F_2 which correspond to each peak in F_1. As discussed in a previous publication,[17] each of these slices through F_2 corresponding to a narrow isotropic line in F_1 will be predominately made up of a single pure-absorption-phase MAS pattern with only minor contributions from additional sites due to overlap in the F_1 dimension. Simulation of the MAS line shape to obtain the quadrupolar parameters C_Q and η is then straightforward, since the line shape depends only upon the fourth-order Legendre polynomial contribution to the second-order quadrupolar interaction. The single-site spectra are fit iteratively by combining a simplex algorithm, such as AMOEBA, described in ref 22, with a high-speed MAS simulation program. The MAS simulation program is based upon a fast simulation method described by Alderman et al.[23] called POWDER. Using a Stardent 750 computer, we can calculate over 1000 spectra in 10 min, thereby facilitating rapid convergence of the simplex routine. The formula which describes the high-speed MAS frequencies as a function of orientation has been given by several authors[4,24-26] and is given in eq 5. The coefficients a_{ij} are given in Table I. This formula may be used to generate an MAS line shape by performing a powder average over all orientations.

$$\delta(\alpha,\beta) = \delta_{obs} - \frac{7 \times 10^6}{64} \frac{C_Q^2(I(I+1) - \frac{3}{4})}{\nu_L^2 I^2 (2I-1)^2} \times$$
$$\left(1 + \frac{\eta^2}{3}\right) \sum_{i=0}^{2} \sum_{j=0}^{2} a_{ij} \cos(2i\alpha) \cos(2j\beta) \quad (5)$$

(22) Press, W. H.; Flannery, B. P.; Teukolsky, S. A.; Vetterling, W. T. *Numerical Recipes: The Art of Scientific Computing*; Cambridge University Press: Cambridge, U.K., 1986.

(23) Alderman, D. W.; Solum, M. S.; Grant, D. M. *J. Chem. Phys.* **1986**, *84*, 3717–3725.

(24) Samoson, A.; Kundla, E.; Lippmaa, E. *J. Magn. Reson.* **1982**, *49*, 350–357.

(25) Lefebvre, F.; Amoureux, J. P.; Fernandez, C.; Derouane, E. G. *J. Chem. Phys.* **1987**, *86*, 6070–6076.

(26) Ganapathy, S.; Schramm, S.; Oldfield, E. *J. Chem. Phys.* **1982**, *77*, 4360–4365.

Frequency (ppm from 1M [87]RbNO$_3$)
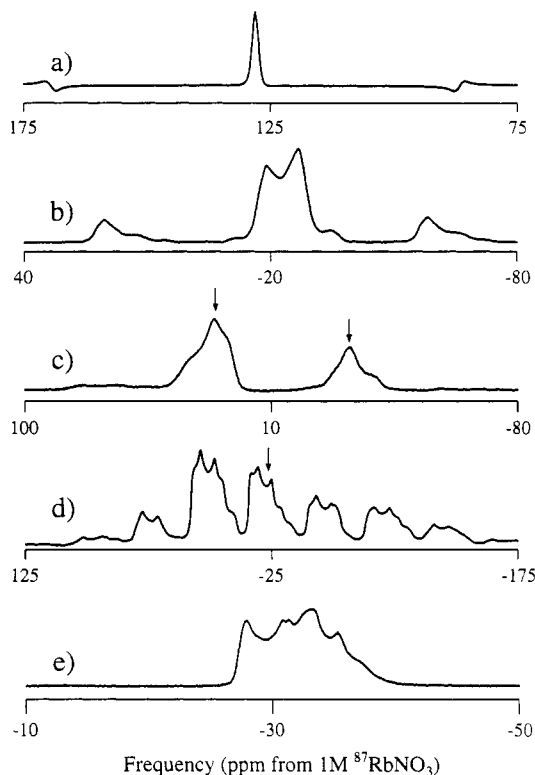
Figure 2. [87]Rb VAS NMR spectra for (a) RbCl at 54.74°, (b) RbClO$_4$ at 54.74°, (c) Rb$_2$SO$_4$ at 79.19°, (d) Rb$_2$CrO$_4$ at 54.74°, and (e) RbNO$_3$ at 54.74° with sweep widths indicated.

Frequency (ppm from 1M [87]RbNO$_3$)
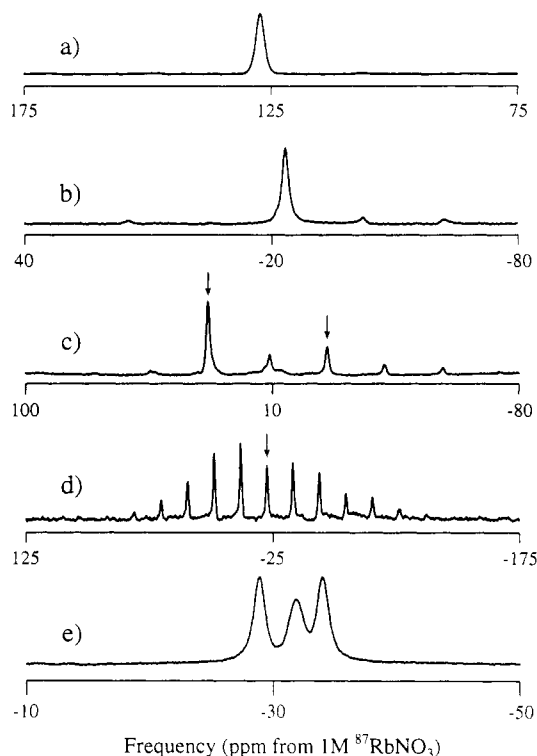
Figure 3. [87]Rb DAS spectra for (a) RbCl, (b) RbClO$_4$, (c) Rb$_2$SO$_4$, (d) Rb$_2$CrO$_4$, and (e) RbNO$_3$ with sweep widths indicated.

Results

Figures 2 and 3 show VAS and DAS spectra of [87]Rb at 11.7 T in RbCl, RbClO$_4$, Rb$_2$SO$_4$, Rb$_2$CrO$_4$, and RbNO$_3$. In all cases except for RbCl, there is narrowing by over an order of magnitude in the high-resolution DAS dimension compared to the MAS spectra. Figure 4 shows the field-dependent shifts of the three lines in RbNO$_3$ upon performing DAS at 4.2, 7.0, 9.4, and 11.7
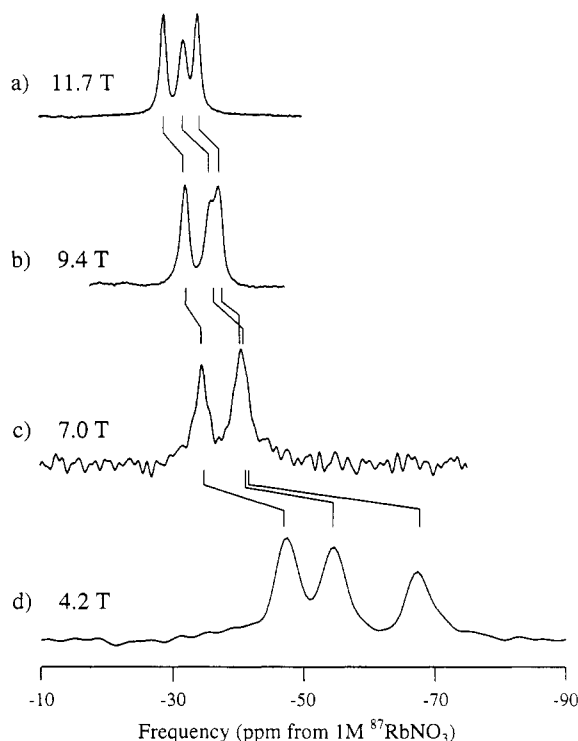
Figure 4. ^{87}Rb DAS spectra of RbNO$_3$ collected at (a) 11.7 T, (b) 9.4 T, (c) 7.0 T, and (d) 4.2 T.

Figure 5. 11.7 T single-site ^{87}Rb MAS spectra of RbNO$_3$ for isotropic peaks at (a) -29 ppm, (b) -32 ppm, and (c) -34 ppm, correlated by means of pure-phase DAS.[17]

Table III. Results from Simulating Single-Site MAS/DAS Spectra at 11.7 T

compd	$\delta_{iso}^{(CS)}$ (ppm)	$C_Q(1 + \eta^2/3)^{1/2}$ (MHz)	C_Q (MHz)	η
RbNO$_3$	-26.2 ± 1.0	1.83 ± 0.05	1.83 ± 0.05	0.12 ± 0.05
	-26.8 ± 1.0	2.39 ± 0.07	2.07 ± 0.05	1.00 ± 0.05
	-30.9 ± 1.0	1.91 ± 0.06	1.85 ± 0.05	0.48 ± 0.05
RbClO$_4$	-16.2 ± 1.0	3.21 ± 0.05	3.20 ± 0.05	0.10 ± 0.05

T. The total isotropic shift at both 9.4 and 11.7 T, the isotropic chemical shift, and the product $C_Q(1 + \eta^2/3)^{1/2}$ calculated from the DAS spectra of the five salts at 9.4 and 11.7 T are tabulated in Table II. Figure 5 shows powder pattern cross sections through the F_2 dimension of a pure-phase MAS-detected ^{87}Rb DAS spectrum at 11.7 T of RbNO$_3$ at the three isotropic frequencies in F_1. Simulations of these three powder patterns are also shown in Figure 5, and the values of $\delta_{iso}^{(CS)}$, C_Q, and η obtained by simulating each site are given in Table III. The quadrupolar parameters obtained by simulating the MAS spectrum of RbClO$_4$ are given in Table III as well. In addition, the quadrupolar parameters determined using a linear fit (shown in Figure 6) of RbNO$_3$ isotropic shifts from four different field strengths are given in Table IV.

T_1's for these compounds ranged from 200 to 300 ms. The T_2 line width of RbNO$_3$ measured with a Carr–Purcell sequence was less than 20 Hz. The line widths measured in the high-resolution F_1 dimension of the DAS spectrum of RbNO$_3$ were 175 Hz, while those in the DOR spectrum of RbNO$_3$ were 80 Hz.

Discussion

The MAS spectrum of RbCl (Figure 2a) gives a slightly narrower line than the DAS spectrum (Figure 3a). This is as expected, since the rubidium nucleus is in an environment of cubic symmetry within the crystal;[11] therefore, there is no second-order
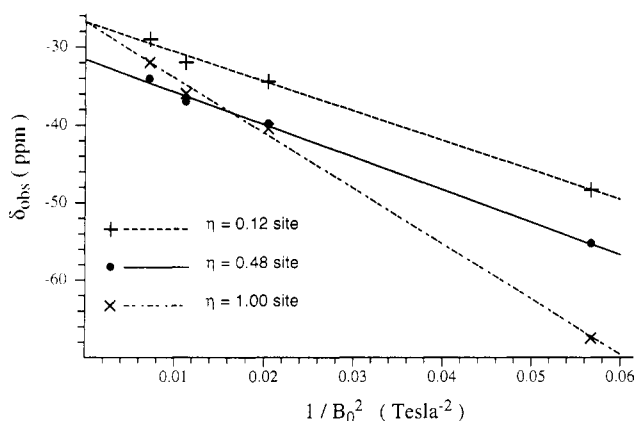
Figure 6. Isotropic shifts (δ_{obs}) of ^{87}RbNO$_3$ plotted versus $1/B_0^2$ and fit using a linear least squares routine. The slopes and intercepts are used to calculate the values of $\delta_{iso}^{(CS)}$ (ppm) and $C_Q(1 + \eta^2/3)^{1/2}$ (MHz).

broadening. Both DAS and MAS will average first-order quadrupolar and chemical shift anisotropy, but as discussed below, only MAS will average the homonuclear dipolar interaction. The additional broadening in the DAS spectrum of RbCl arises from the scaled homonuclear dipolar interaction.

The MAS spectrum of RbClO$_4$ (Figure 2b) yields a well-resolved powder pattern which may be simulated quite easily (Table III). These simulations agree completely with the isotropic chemical shift and quadrupolar parameters determined by the DAS measurements (Figure 3a) at the two different fields.

The ^{87}Rb VAS 79.19° spectrum of Rb$_2$SO$_4$ (Figure 2c) shows that two powder patterns centered at -18 and 33 ppm can be resolved. The 79.19° spectrum is shown instead of the MAS spectrum because the 79.19° spectrum is significantly narrower. These lines narrow substantially under DAS (Figure 3c) to give two sharp peaks corresponding to the two crystallographically distinct Rb sites in this compound. One of these resonances is clearly present at $\delta_{obs}^{11.7T}$ = 34 ppm, while the upfield site is broken into spinning sidebands. Assignments of the line at $\delta_{obs}^{11.7T}$ = -10 ppm to the isotropic resonance position of the second site was made by comparing DAS spectrum taken at spinning speeds of 5.3 and 6.5 kHz. This also demonstrates that the actual isotropic shift of a VAS powder pattern is not necessarily the most intense point of the VAS spectrum.

Table IV. Results from a Linear Least Squares Fit of the Isotropic Shifts as a Function of $1/B_0^2$ for RbNO$_3$

$\delta_{obs}^{4.2T}$ (ppm)	$\delta_{obs}^{7.0T}$ (ppm)	$\delta_{obs}^{9.4T}$ (ppm)	$\delta_{obs}^{11.7T}$ (ppm)	$\delta_{iso}^{(CS)}$ (ppm)	$C_Q(1 + \eta^2/3)^{1/2}$ (MHz)
-48.4 ± 1.0	-34.4 ± 1.0	-32.0 ± 1.0	-29.0 ± 1.0	-26.8 ± 0.8	1.72 ± 0.06
-67.5 ± 1.0	-39.8 ± 1.0	-36.0 ± 1.0	-32.0 ± 1.0	-26.8 ± 0.8	2.36 ± 0.04
-55.3 ± 1.0	-40.2 ± 1.0	-37.0 ± 1.0	-34.0 ± 1.0	-31.6 ± 0.8	1.81 ± 0.05

The DAS (Figure 3d) and MAS (Figure 2d) spectra of Rb_2CrO_4 show a single site with prominent sets of spinning sidebands. The isotropic line was assigned by performing DAS at two different spinning speeds. However, there are two crystallographically distinct Rb sites in Rb_2CrO_4.[13] The large C_Q ($\sim$12 MHz) for the second site[10] makes it unobservable because the total intensity is distributed over a bandwidth that is too broad to be excited with 5 μs rf pulses.

The MAS spectrum of $RbNO_3$ (Figure 2e) consists of three overlapping powder patterns, which give rise to narrow, resolved lines under DAS (Figure 3e). The MAS spectra extracted from the phase-sensitive DAS spectrum were fit by computer simulations, each simulation starting with a different set of initial parameters covering a wide range of values. All simulations converged to the same set of parameters within $\pm0.01\%$. Our estimates for the absolute accuracy of the simulations are that C_Q is accurate to ±0.05 MHz, η to ±0.05, and the isotropic chemical shift to ±1.0 ppm. These error estimates are shown in Table III.

Calculation of the product $C_Q(1 + \eta^2/3)^{1/2}$ and the isotropic chemical shift, $\delta_{iso}^{(CS)}$, using data from DAS spectra taken at two different field strengths and eq 4 can introduce large errors, since this requires two DAS measurements and two external references. Furthermore, since $C_Q(1 + \eta^2/3)^{1/2}$ is proportional to the square root of the difference between the two isotropic shifts at two different fields, smaller differences lead to larger errors. The actual error analysis is straightforward, and we report overall errors in Table II for all calculated parameters assuming that the measurements are accurate to ±1 ppm. Since the errors of the parameters determined by simulation of a single site can be less than those determined by two field measurements, it is highly desirable to perform simulations in conjunction with the measurements at two or more magnetic field strengths.

Performing measurements at four different magnetic field strengths greatly improves the accuracy and precision of the calculated product $C_Q(1 + \eta^2/3)^{1/2}$ and $\delta_{iso}^{(CS)}$. This has been done with $RbNO_3$ by comparing the results from this work with measurements taken at 4.2 T.[27] We observe a linear relationship between δ_{obs} and $1/B_0^2$ for each of the three sites as predicted (Figure 6). The slope of each line may be related to $C_Q(1 + \eta^2/3)^{1/2}$ by eq 4, while the zero intercept (which corresponds to infinite field) is simply $\delta_{iso}^{(CS)}$. Also a linear least squares analysis allows estimation of errors, and we observe a dramatic improvement over two-field results (almost a factor of 10). This improvement arises due to the large range of isotropic shift differences between the measurements at all four fields. The results and errors are compiled in Table IV and agree very well with our simulations.

The isotropic shift for RbCl that we report is in very good agreement with the work by Cheng et al.,[10] indicating that our external references were consistent with theirs, but our determination of the isotropic chemical shifts for the other salts using DAS is different. We expect DAS to give more precise values than wide-line simulation techniques, which require a large number

of adjustable parameters, since DAS allows the determination of isotropic chemical shifts and $C_Q(1 + \eta^2/3)^{1/2}$ directly. Furthermore, in the case of $RbNO_3$, DAS allows us to separate MAS powder patterns and determine isotropic chemical shifts, quadrupolar coupling constants, and asymmetry parameters for each of the $RbNO_3$ sites through single-site simulation. The quadrupolar parameters determined for $RbNO_3$ by multiple-field DAS measurements agree quite well with a previous study performed in a low magnetic field by Segel.[28]

It is interesting to note that while the width of the lines in the DAS spectrum of $RbNO_3$ is 175 Hz, the width of those in the DOR spectrum is only 80 Hz. This difference arises in part from the fact that homonuclear dipole–dipole coupling is averaged more completely by DOR than by DAS. Multilinear homonuclear terms (e.g. $I_{1+}I_{2z}...I_{nz}$) created during the first $t_1/2$ period of the DAS experiment are not stored by the second $\pi/2$ pulse and hence decay during the hop and cannot be refocused in the second $t_1/2$ period. Therefore, in order for a DAS experiment to give narrow lines, the homonuclear dipolar coupling must be small. However, this residual broadening can be minimized by using the $k = 5$ solution for the DAS angles rather than $k = 1$, where k is defined in ref 3.

T_1 relaxation times for $RbNO_3$ and Rb_2SO_4 are both in the range 200–300 ms, in agreement with those previously reported by Cheng et al.[10] These T_1's are ideal for DAS, as they require a minimum delay for complete T_1 relaxation between scans, but at the same time, the signal does not decay unduly during the hop(s) (30 ms/hop). In addition, the observed isotropic chemical shift range for these compounds is quite large (over 150 ppm), significantly larger than that observed for similar sodium compounds. This is due to the larger electron cloud surrounding a rubidium nucleus leading to a larger polarizability.

Finally, we note that there are two NMR-active isotopes of rubidium, ^{85}Rb ($I = {}^5/_2$) and ^{87}Rb ($I = {}^3/_2$). We have obtained ^{85}Rb DAS spectra of some of the compounds, but ^{87}Rb gives DAS spectra superior to those of ^{85}Rb, since the sensitivity of ^{87}Rb is greater and its relaxation time longer. ^{87}Rb has the disadvantage that the residual homonuclear dipolar broadening of the DAS line is larger, but, in our experience, spectroscopy of ^{87}Rb appears to be advantageous, especially in cases where C_Q is between 1.0 and 8.0 MHz.

(27) Grandinetti, P. J.; Baltisberger, J. H.; Llor, A.; Lee, Y. K.; Werner, U.; Eastman, M. A.; Pines, A. *J. Magn. Reson.*, submitted for publication.

(28) Segel, S. L. *J. Chem. Phys.* **1980**, *73*, 4146–4147.